J|A|C|S ARTICLES

Published on Web 02/24/2010

# Synthesis of Monodisperse PbSe Nanorods: A Case for Oriented Attachment

Weon-kyu Koh,[†] Adam C. Bartnik,[§] Frank W. Wise,[§] and Christopher B. Murray*[,†,‡]

*Department of Chemistry and Department of Materials Science and Engineering, University of Pennsylvania, Philadelphia, Pennsylvania 19104, and School of Applied and Engineering Physics, Cornell University, Ithaca, New York 14853*

Received December 15, 2009; E-mail: cbmurray@sas.upenn.edu

***Abstract:*** Monodisperse, high-quality, single-crystal PbSe nanorods were synthesized in a catalyst-free, one-pot reaction using a new phosphine selenide precursor. PbSe nanorods were assembled to provide liquid-crystalline alignment or vertical alignment under controlled evaporation conditions. The growth of nanorods was monitored by TEM and absorption spectroscopy, indicating that oriented attachment could be involved to provide anisotropic PbSe nanostructures. In-plane XRD showed an enhanced (200) peak for PbSe nanorods, indicating the preferred alignment of nanorods on the substrates and their growth along the ⟨100⟩ direction. Absorption and emission spectra, along with lifetime measurements, show the differences between nanoscale PbSe spheres and rods.

## Introduction

The solution-process synthesis of nanocrystals (NCs) has been developed intensively for electronic, optical, and magnetic applications.[1−3] In particular, the ability to control the morphology of semiconductor NCs has presented many research opportunities in understanding the fundamental properties of materials and developing electro-optical devices.[4−9]

Lead selenide (PbSe) is a narrow band gap (0.28 eV, bulk) material that has small effective masses for both holes and electrons (∼0.1 $m_o$) and a large exciton Bohr radius (23 nm).[10,11] Although PbSe is interesting in semiconductor and IR applications, especially when its size and morphology can be controlled on the nanoscale, there have been few reports of anisotropic PbSe nanostructures. Previously, Cho et al. reported PbSe nanowires (NWs) made by oriented attachment,[12] a process that makes anisotropic nanostructures from individual particles by joining them to high-energy surfaces.[13−15] In their paper, PbSe nanowires were synthesized at a higher temperature (250 °C) than PbSe NCs (150−170 °C) in order to enhance oriented attachment and to produce longer NWs; the authors also used tetradecylphosphonic acid or hexadecylamine as a cosurfactant to control the morphology of wires (straight or zigzag shape). However, optical properties of NWs are not easy to study because of the low NW solubility and large scattering, especially when surface traps exist. In addition, rapid wire formation (<1 min) at high temperature has prevented the detailed understanding of oriented attachment in the growth of PbSe structures and has also made it difficult to modify the morphology and size of NWs. There have been other reports of anisotropic lead chalcogenide nanostructures, such as PbSe nanorods (NRs) using Au−$Fe_3O_4$ seeds,[16] PbSe NWs using a Au/Bi catalyst,[17] and PbS NRs using cationic exchange on CdS NRs,[18] but none of them have shown a catalyst-free, one-pot synthesis of single-crystalline, anisotropic PbSe nanostructures.

Here we report a simple, high-quality PbSe NR synthesis and their shape-dependent structural/optical properties. The key improvement reported here is controlled NR growth enabled by the use of tris(diethylamino)phosphine selenide (TDPSe) instead of trioctylphosphine selenide (TOPSe). This makes possible the NR growth of PbSe at lower temperatures on a

[†] Department of Chemistry, University of Pennsylvania.
[‡] Department of Materials Science and Engineering, University of Pennsylvania.
[§] Cornell University.

(1) Murray, C. B.; Kagan, C. R.; Bawendi, M. G. *Annu. Rev. Mater. Sci.* **2000**, *30*, 545–610.
(2) Sun, S. H.; Murray, C. B.; Weller, D.; Folks, L.; Moser, A. *Science* **2000**, *287*, 1989–1992.
(3) Wang, H.; Brandl, D. W.; Nordlander, P.; Halas, N. J. *Acc. Chem. Res.* **2007**, *40*, 53–62.
(4) Scher, E. C.; Manna, L.; Alivisatos, A. P. *Philos. Trans. R. Soc. London, Ser. A* **2003**, *361*, 241–255.
(5) Sigman, M. B.; Ghezelbash, A.; Hanrath, T.; Saunders, A. E.; Lee, F.; Korgel, B. A. *J. Am. Chem. Soc.* **2003**, *125*, 16050–16057.
(6) Wang, W.; Banerjee, S.; Jia, S. G.; Steigerwald, M. L.; Herman, I. P. *Chem. Mater.* **2007**, *19*, 2573–2580.
(7) Yu, H.; Li, J.; Loomis, R. A.; Gibbons, P. C.; Wang, L.-W.; Buhro, W. E. *J. Am. Chem. Soc.* **2003**, *125*, 16168–16169.
(8) Huynh, W. U.; Dittmer, J. J.; Alivisatos, A. P. *Science* **2002**, *295*, 2425–2427.
(9) Gur, I.; Fromer, N. A.; Chen, C. P.; Kanaras, A. G.; Alivisatos, A. P. *Nano Lett.* **2007**, *7*, 409–414.
(10) Kang, I.; Wise, F. W. *J. Opt. Soc. Am. B* **1997**, *14*, 1632–1646.
(11) Du, H.; Chen, C. L.; Krishnan, R.; Krauss, T. D.; Harbold, J. M.; Wise, F. W.; Thomas, M. G.; Silcox, J. *Nano Lett.* **2002**, *2*, 1321–1324.
(12) Cho, K. S.; Talapin, D. V.; Gaschler, W.; Murray, C. B. *J. Am. Chem. Soc.* **2005**, *127*, 7140–7147.
(13) Penn, R. L.; Banfield, J. F. *Science* **1998**, *281*, 969–971.
(14) Tang, Z. Y.; Kotov, N. A.; Giersig, M. *Science* **2002**, *297*, 237–240.
(15) Pacholski, C.; Kornowski, A.; Weller, H. *Angew. Chem., Int. Ed.* **2002**, *41*, 1188–1191.
(16) Yong, K. T.; Sahoo, Y.; Choudhury, K. R.; Swihart, M. T.; Minter, J. R.; Prasad, P. N. *Nano Lett.* **2006**, *6*, 709–714.
(17) Hull, K. L.; Grebinski, J. W.; Kosel, T. H.; Kuno, M. *Chem. Mater.* **2005**, *17*, 4416–4425.
(18) Luther, J. M.; Zheng, H. M.; Sadtler, B.; Alivisatos, A. P. *J. Am. Chem. Soc.* **2009**, *131*, 16851–16857.

  

longer timescale (150−170 °C, >2 to 3 min), so we could monitor a transition process of NR growth by TEM and absorption spectra. Details of the synthesis, along with structural analysis and optical properties of the PbSe NRs, will be presented.

## Experimental Section

**Chemicals.** All manipulations were carried out using standard Schlenk-line techniques under dry nitrogen. Tris(diethylamino)-phosphine (TDP, Aldrich, 97%), oleic acid (OA, Aldrich, 90%), 1-octadecene (ODE, Aldrich, 90%), squalane (Aldrich, 99%), amorphous selenium shots (Se, Aldrich, 99.999%), and lead(II) oxide (PbO, Aldrich, 99.9%) were used as purchased without further purification. Anhydrous ethanol, chloroform, acetone, hexane, and tetrachloroethylene (TCE) were purchased from various sources. To prepare 1.0 M stock solutions of TDPSe, 7.86 g of Se was dissolved in 100 mL of TDP.

**Synthesis of PbSe Nanorods.** Typically, 0.22 g of PbO was dissolved in 5 mL of squalane in the presence of 1 mL OA. (Squalane can be replaced by ODE.) After drying under nitrogen at 150 °C for 30 min, the solution was heated to 170 °C and 3 mL of a 1 M TDPSe solution in TDP was injected under vigorous stirring. Once the reaction finished, the reaction mixture was cooled to room temperature using a water bath. The crude solution was mixed with hexane and precipitated by ethanol. The precipitated NRs were isolated by centrifugation (at 5000 rpm for 3 min) and redispersed in chloroform or other organic solvents. Size-selective precipitation can be carried out to obtain better monodispersity of NRs samples using chloroform/acetone or other solvent/nonsolvent pairs.

**Sample Characterization.** Powder X-ray diffraction (XRD), in-plane XRD, and transmission small-angle X-ray scattering (TSAXS) were performed using Cu $K\alpha_1$ radiation ($\lambda = 1.54$ Å) from a Rigaku SmartLab at 40 kV and 30 mA. For XRD measurement, samples were prepared by depositing NCs or NRs solutions in hexane onto a Si substrate or a glass plate. For in-plane XRD measurement, the incident angle was typically 0.83°. For TSAXS measurement, the 1 mm capillaries containing the NR solutions (∼5% in toluene) were sealed and mounted perpendicularly to the beam direction. The TSAXS fitting curve was simulated using NANO-Solver (Rigaku software). Transmission electron microscopy (TEM), high-resolution TEM, and energy-dispersive X-ray spectroscopy (EDX) were carried out by using a JEOL JEM 1400 and a 2010F at 120 and 200 kV, respectively. Samples for TEM images were prepared by dropping a solution onto a 300 mesh carbon-coated copper grid and allowing the solvent to evaporate at room temperature. Absorption spectra were measured on a Shimadzu UV-3101PC spectrophotometer at room temperature. Emission spectra were recorded at room temperature with an infrared fluorometer equipped with a 200 mm focal length monochromator, a single-mode fiber-coupled laser (S1FC635PM, 635 nm, Thorlabs, Inc.) as the excitation source, and an InGaAs photodiode detector (New Focus

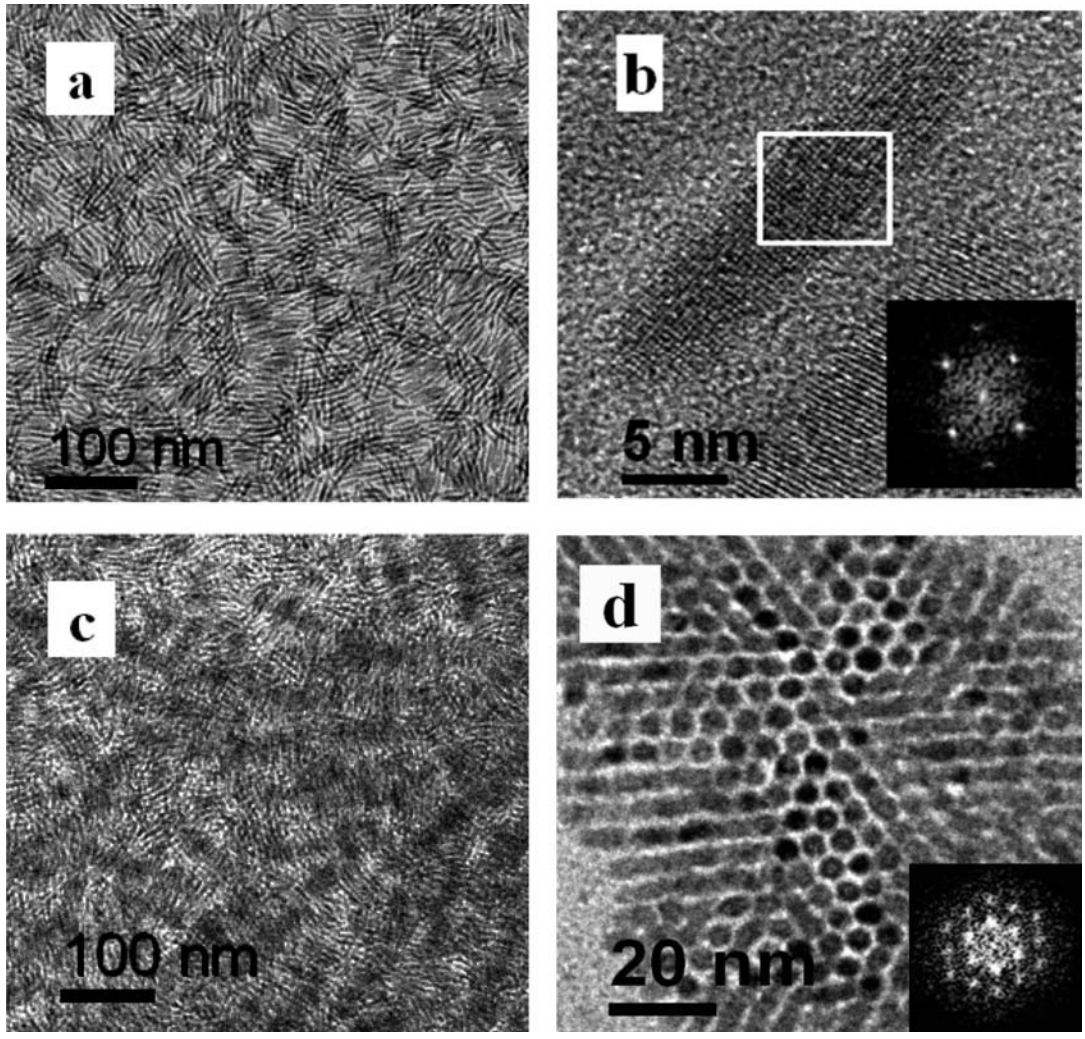


***Figure 1.*** (a) TEM image of typical PbSe NRs. (b) High-resolution TEM image of an individual PbSe NR. (Inset: FFT image of the (100) face.) (c) Liquid-crystalline assembly of PbSe NRs. (d) Vertical alignment of shorter PbSe NRs. (Inset: FFT image of hexagonally assembled NRs.)

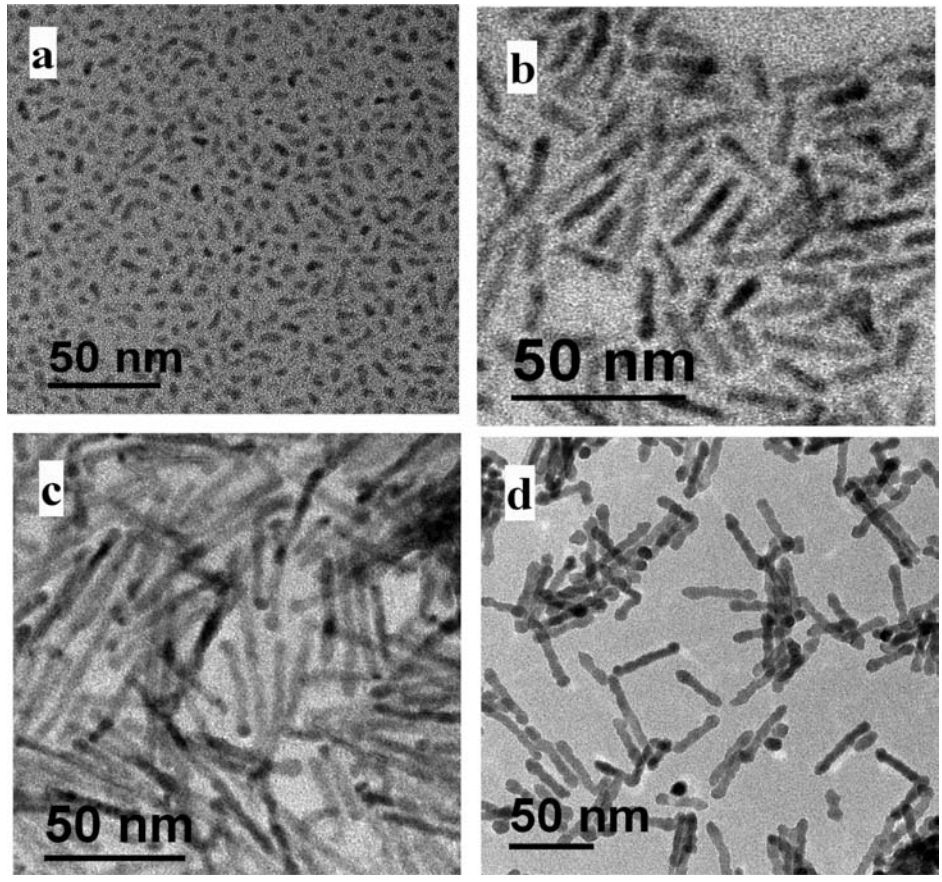


***Figure 2.*** TEM images of different growth times: (a) 30 s, $d = 3.9$ nm; (b) 2 min, $d \times L = 3.8 \times 21$ nm$^2$; (c) 4 min, $d \times L = 4.1 \times 44$ nm$^2$; and (d) 8 min, $d \times L = 5.7 \times 35$ nm$^2$. ($d$ is the diameter of the rods, and $L$ is the length of the rods.) At stage d, the actual products are a polydisperse mixture of rods and particles, so it is not suitable to compare the average length with that of other samples.

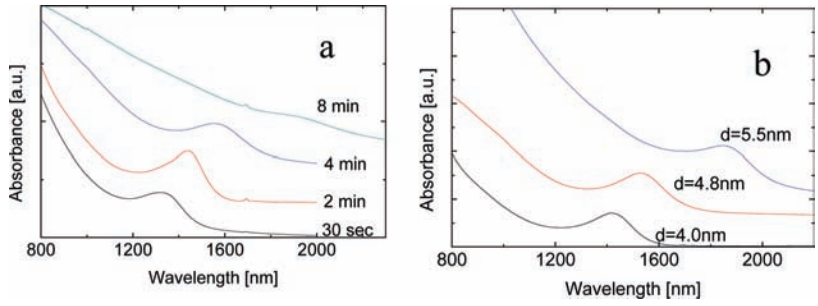


***Figure 3.*** Absorption spectra of (a) different growth times (the same conditions as shown in Figure 3) and (b) different diameters of PbSe NRs. (Diameter/length of the samples shown in plot b = $4.0 \times 16$ nm$^2$, $4.8 \times 26$ nm$^2$, and $5.5 \times 41$ nm$^2$.)

Femtowatt model 2153). The samples were excited at a repetition rate of 20 kHz by nanosecond pulses of a Lumanova muFlare laser system frequency doubled to 532 nm. The sample was exposed to intensity levels well below one electron−hole pair per dot. Fluorescence was monitored with a Hamamatsu H10330A-75 PMT, and the output was fed into and averaged by a 1 GHz oscilloscope. All optical experiments were carried out in TCE solvent.

## Results and Discussions

**Synthesis of PbSe Nanorods, Assemblies, and Growth Transition.** Figure 1a shows a TEM image of typical PbSe NR with ~4 and 40 nm diameter and length, respectively. As shown in Figure 1b, the rod is single-crystalline; here we can see the {100} facet, which is matched with the inset Fourier transform image. Interestingly, slow evaporation of PbSe NR solutions in chloroform or TCE allowed liquid-crystalline assembly (Figure 1c) and vertical alignment (Figure 1d), as shown in previous reports of CdSe NRs.[19,20] To investigate the process of PbSe NR growth, an aliquot of the reaction solution was taken at different time points and observed by TEM. At first, small particles were produced from the mixing of lead and selenide precursors (Figure 2a). Later, the aspect ratio increased rapidly but the diameter increased slowly (Figure 2b,c). This can be confirmed by absorption spectra during rod growth in which the first exciton peak was shifted only slightly (Figure 3a). This corresponds to a slow increase in rod diameter because the quantum confinement effect of anisotropic nanostructures mostly depends on the smallest length scale present. An example

(19) Li, L. S.; Alivisatos, A. P. *Adv. Mater.* **2003**, *15*, 408–411.
(20) Ryan, K. M.; Mastroianni, A.; Stancil, K. A.; Liu, H. T.; Alivisatos, A. P. *Nano Lett.* **2006**, *6*, 1479–1482.

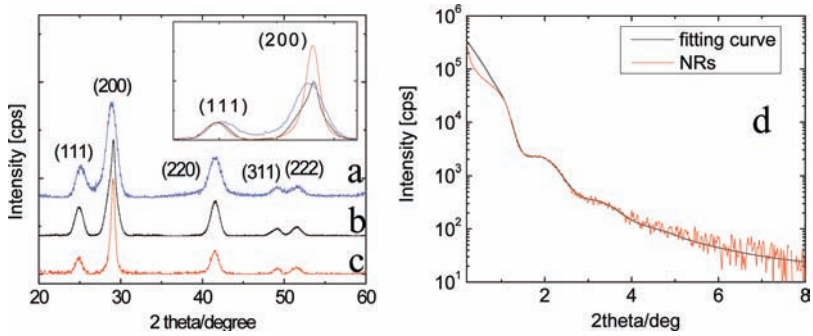


***Figure 4.*** (a) WAXS pattern of PbSe NCs. (b) WAXS pattern of PbSe NRs. (c) In-plane XRD pattern of PbSe NCs. (Inset: magnified XRD patterns of (111) and (200) peaks for a−c; patterns normalized to the (111) peak.) (d) TSAXS pattern of NRs with a fitting curve.

of this is the case of CdTe tetrapods with a similar length that showed diameter-dependent first exciton peak positions whereas samples with fixed diameter showed almost identical first peak positions regardless of the length of the tetrapod branches.[21] Another example is the case of PbSe NRs, for which samples with various diameters confirm that the first peak of the absorption spectrum depends mainly on the NR diameter (Figure 3b). After the reaction time represented in Figure 2c, the surface of the rods was rough and the products were polydisperse (Figure 2d). As reported in a previous paper,[12] the rapid transition from small particles (Figure 2a) to NRs (Figure 2b) and attached particles or wires (Figures S1 and S2) implies the possible mechanism of oriented attachment. This would occur in addition to Ostwald ripening, a commonly observed process in nanocrystalline semiconductor synthesis (Figure 2c,d).

**Structural Analysis Using in-Plane XRD and TSAXS.** In wide-angle X-ray scattering (WAXS), the diffraction peaks of PbSe NRs showed good agreement with those of spherical PbSe NCs, except for a slightly narrower (200) peak (Figure 4a,b). On a flat Si wafer, there is likely a similar mixture of NR orientations as observed on a TEM substrate. This mixture of orientations (standing up, lying down, and intermediate) gives rise to a diffraction pattern that reflects collective isotropy that is similar to that of individual PbSe spheres. However, because NRs are elongated, more of the NRs align parallel to the substrate than vertically (as shown in Figure 1c,d). To confirm the anisotropy of PbSe NRs, we performed in-plane XRD on the same sample as used in Figure 4b and saw an enhanced (200) peak. This implies that NR growth is mainly in the ⟨100⟩ direction because an enhanced peak results from an increased number of lattice planes under the Bragg condition for diffraction (Figure 4c). Thus, an enhanced (200) peak can be understood in terms of NR growth in a favored direction and subsequent alignment on the substrate. This growth direction matches the result from a previous report in which PbSe straight nanowires showed only (200) and (220) peaks in XRD.[12] Transmission small-angle X-ray scattering (TSAXS) was also performed on PbSe NRs that were dispersed in toluene and then loaded into a capillary tube. The data in Figure 4d was fitted to a cylindrical model with a 6.8 nm diameter and an aspect ratio of 3.5. (The size of the NRs is $6 \times 18$ nm$^2$ (diameter $\times$ length), as measured by TEM.) The PbSe NR SAXS data deviate from the cylindrical model for angles below $2\theta = 1.0°$, most likely because of short-range correlations between NRs for the relatively concentrated conditions under which the SAXS measurements were made. These short-range correlations between NRs are similar to Jana's report that Au NRs form small clusters under SAXS measurement conditions.[22]

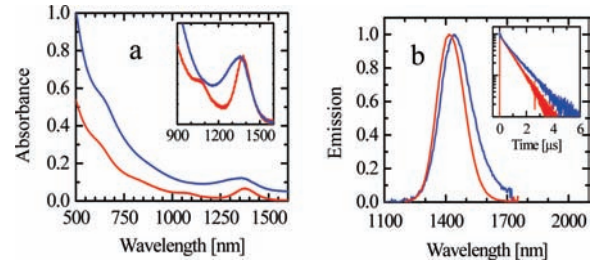


***Figure 5.*** (a) Absorption of PbSe NRs (blue, *y* axis offset for clarity) and NCs (red); the inset shows the detail of the first exciton peak. (b) Normalized PL of NRs (blue) and NCs (red); the inset shows the time dependence measured at the PL peak of each sample. The NCs and NRs in this study have similar diameters.

**Optical Properties of PbSe Nanorods.** To characterize the optical properties of the NRs, we measured their absorption, photoluminescence (PL), transient PL, and quantum yield (QY), and the same optical characterization was performed on spherical PbSe NCs of the same diameter for comparison. Figure 5 shows the optical spectra of a characteristic sample of the NCs and NRs, chosen to have similar absorption peaks. To the best of our knowledge, this study represents the first optical characterization of monodisperse PbSe NRs and thus provides the first opportunity to compare their well-resolved excitonic transitions with those of spherical PbSe NCs. The NRs show a well-defined first excitonic absorption peak at around 1360 nm and an emission peak at 1440 nm, compared to a NC absorption at 1375 nm and emission at 1420 nm. This larger Stokes shift was typical of all measured samples, which in general had a noticeably larger shift (~2- to 3-fold) than similar-diameter NCs. Both NRs and NCs have approximately microsecond lifetimes, with the NRs being slightly longer at 1.1 $\mu$s. These are similar to the larger Stokes shift and longer lifetimes exhibited by CdSe NRs, as compared to those of CdSe NCs.[23,24] Beyond the first absorption peak, the NRs show a less-structured absorption spectrum with fewer discernible peaks. In addition, whereas the low-energy half of the first exciton peak share the same width for both samples, the high-energy side of the NRs is significantly broader. The fluorescence QY of the NRs is approximately 15%, measured using an integrating sphere, which is similar to

(21) Milliron, D. J.; Gur, I.; Alivisatos, A. P. *MRS Bull.* **2005**, *30*, 41–44.
(22) Jana, N. R.; Gearheart, L. A.; Obare, S. O.; Johnson, C. J.; Edler, K. J.; Mann, S.; Murphy, C. J. *J. Mater. Chem.* **2002**, *12*, 2909–2912.
(23) Hu, J. T.; Li, L. S.; Yang, W. D.; Manna, L.; Wang, L. W.; Alivisatos, A. P. *Science* **2001**, *292*, 2060–2063.
(24) Wang, X. Y.; Zhang, J. Y.; Nazzal, A.; Darragh, M.; Xiao, M. *Appl. Phys. Lett.* **2002**, *81*, 4829–4831.

commonly reported QYs of 20−40% for PbSe NCs,[25] and it is possible that this could be improved in a manner similar to that for the PbSe/CdSe core/shell NCs recently reported.[26] Interestingly, CdSe NRs show quite low QYs of 0.6% without shell passivation, presumably because of dense surface traps, whereas a CdS/ZnS shell enhanced the QY of CdSe NRs up to 16%.[27] Compared to that of CdSe NRs, the QY of PbSe NRs is remarkably high, implying that these NRs are high quality even without shell passivation. A more detailed mechanism of PbSe NR formation and a theoretical/spectroscopic analysis of shape-dependent PbSe nanostructures will be presented in upcoming work.

## Conclusions

We report a simple, one-pot, catalyst-free synthesis of high-quality PbSe NRs, confirmed by TEM and X-ray analysis. Optical spectroscopy shows the shape-dependent anisotropic behavior of PbSe NRs as compared to that of spherical NCs (i.e., a larger Stokes shift and longer fluorescence lifetime). Because there are many unresolved questions about the properties of PbSe nanostructures (e.g., carrier multiplication and intraband transitions), we hope that this study will open up new research opportunities.

**Acknowledgment.** We acknowledge financial support from the NSF through DMS-0935165 (C.B.M. and W.-k.K.), which enabled the detailed structural x-ray and electron microscopy studies, and from the Center for Nanoscale Systems through the Nanoscale Science and Engineering Initiative of the National Science Foundation, award number EEC-0117770 (A.C.B. and F.W.W.). This research was partially supported by the Nano/Bio Interface Center through the National Science Foundation (NSEC DMR08-32802) with a seed grant that initiated the synthesis investigation of the nanorods. We thank Douglas M. Yates and Lolita Rotkina of the Penn Regional Nanotechnology Facility at the University of Pennsylvania for support in electron microscopy. W.-k.K. thanks Prof. P. A. Heiney for help with the TSAXS experiment and Danielle Reifsnyder for editing the manuscript.

**Supporting Information Available:** Supplementary figures as described in the text. This material is available free of charge via the Internet at http://pubs.acs.org.

JA9105682

(25) Steckel, J. S.; Coe-Sullivan, S.; Bulovic, V.; Bawendi, M. G. *Adv. Mater.* **2003**, *15*, 1862–1866.
(26) Pietryga, J. M.; Werder, D. J.; Williams, D. J.; Casson, J. L.; Schaller, R. D.; Klimov, V. I.; Hollingsworth, J. A. *J. Am. Chem. Soc.* **2008**, *130*, 4879–4885.
(27) Manna, L.; Scher, E. C.; Li, L. S.; Alivisatos, A. P. *J. Am. Chem. Soc.* **2002**, *124*, 7136–7145.